SIMULATING URBAN HEAT ISLAND EFFECTS USING AN URBAN SCHEME COUPLED WITH GLOBAL CLIMATE/LAND-SURFACE MODELS

MENGLIN JIN AND CHRISTA D. PETERS-LIDARD

Short title: An Urban Scheme for Land Surface Models

Journal of Hydrometeorology
(Manuscript 2005)

Authors Dr. Menglin Jin*
Climate and Radiation Branch
NASA-GSFC Code 613.2
Greenbelt, Maryland 20771
Department of Meteorology
University of Maryland, College Park
301-614-6186
mjin@atmos.umd.edu

Dr. Christa Peters-Lidard
Hydrological Sciences Branch
NASA-GSFC Code 614.3
Greenbelt, Maryland 20771
301-614-5811
Christa.D.Peters-Lidard@nasa.gov

Abstract

Urbanization is an extreme case of human-induced land cover and use change. Simulating urbanization-induced climate change, in particular, the urban heat island effect (UHI), is critical for realistically representing urban regions in the land surface-atmosphere climate system. However, including urban landscapes in regional or global climate models has been overlooked due to the coarse spatial resolution of these models as well as the lack of observations for urban physical properties. For example, no urbanization has been included in the leading U.S. global modeling systems at the National Center for Atmospheric Research (NCAR), The National Centers for Environmental Prediction (NCEP) and the National Aeronautics and Space Administration (NASA). Recently, NASA satellite Earth Observing System (EOS) Moderate Resolution Imaging Spectroradiometer (MODIS) observations illustrate important urban physical properties, including skin temperature, surface albedo, surface emissivity, and leaf area index, For the first time, it is possible to identify the unique urban features and thus simulate global urban processes .

An urban scheme is designed to represent the modified physical parameters (albedo, emissivity, land cover, roughness length, thermal and hydraulic properties) and to include new, unique physical processes that exist in urban regions. The urban scheme is coupled with NCAR Community Land Model Version 2 (CLM2) and single column coupled NCAR Community Atmosphere

Model CAM2/CLM2 to assess the mechanisms responsible for UHI. There are two-steps in our model development. First, satellite observations of albedo, emissivity, LAI, and *in situ* observed thermal properties are updated in CLM2 to represent the first-order urban effects. Second, new terms representing the urban anthropogenic heat flux, storage heat flux, and roughness length are calculated in the model. Model simulations suggest that human activities decrease urban surface albedo and emissivity, enhance overlying atmospheric instability and convective rainfall, and eventually result in urban heat island effect**.**

1. Introduction

The most recent Intergovernmental Panel on Climate Change report (IPCC 2001) confirms that "there is new and stronger evidence showing that most of the warming observed over the last 50 years is attributed to human activities." Although IPCC (2001) is focused on human-induced greenhouse gas impacts, another human impact, urbanization, also worthy of special attention due to its rapid associated changes in land cover and use (Oke 1982, Landsberg 1980, Karl et. al. 1988, Grimmond and Oke 1999, Hansen et. al. 2000, Shepherd et. al. 2003, Jin et al. 2005a, Shepherd and Jin 2005).

GCMs coupled with land surface models have been considered one of the most useful tools to examine land cover change impacts on the climate system, and to project future changes (Manabe 1968, Dickinson and Shenider 1977, Avissar and Pielke 1989, Dickinson 1992, IPCC 2001). The land surface model in a GCM simulates terrestrial water, energy and biogeochemical processes as well as the transfers of heat, mass and momentum between the land surface and the overlying atmosphere model. Unfortunately, simulating urban effects is one of the weakest aspects of current land surface models, because most were developed from the perspective of coarse-resolution (e.g., about 1 degree) global models within which urban processes and impacts were thought to be unimportant. Further, understanding of urban properties and physical processes remains incomplete. Previous research studied one or a few selected cities (Karl 1988, Huff and Vogel 1978, Changnon 1978, Brest 1987, Shepherd and Brain 2003, Brian and Shepherd 2004, Jin et al. 2005b). Urban effects, however, vary with the micro-scale features of each individual city (Oke 1976, 1982 Jin et al, 2005a, b) .Since urban climate closely influences people's daily lives, it needs to be precisely understood and predicted (Changnon 1992). Beyond the specific

challenges of urban properties and processes, we lack a full understanding of land surface-atmosphere interaction. Previous results, via different approaches, were controversial. For example, some studies reported that urban areas reduced rainfall due to cloud microphysics (Ramanathan et al. 2001), while other studies showed that urban areas significantly enhanced the intensity of storm and increased downward rainfall (Huff and Vogel 1978, Changnon 1978, Shepherd et. al. 2002). These present the challenges in simulating urban landscape in a GCM/land surface model.

Consequently, urban landscapes have not been included in the current generation of land surface models, and therefore simulations of urban impacts have been largely absent from the literature (Jin and Shepherd, 2004). All the leading U.S. land surface models, including NCAR's CLM2 (Oleson et. al. 2004), the developing NASA unified land surface model (Randy Koster, personal communication 2004), and NCEP's Noah land surface model (Ek et al, 2003; Mitchell, personal communication, 2004) have not yet included urban parameterizations in their models when the present model was developed.

Our work aims to develop an urban scheme to enhance currently existing land surface models for better simulating urbanization, by combining recently available EOS satellite observations and results from previous studies based largely on field experiments (Oke 1982, Grimmand and Oke 1999, King et. al. 2003, Shepherd and Brian 2003, Jin et. al. 2004 a,b). Specifically, we hope to shed light on three key questions: (1) What are the physical mechanisms responsible for the urban heat island effect? (2) What is the relative importance of the mechanisms? (3) Are there any unique features related to urban land surface-atmosphere interactions?

As the first version of our urban model, we focus only on simulating land

surface energy budgets and purposely ignore other processes including momentum changes over urban buildings. A detailed model for simulating urban impacts on momentum exchange is given by Otte et al. (2004). We also neglect urban induced atmospheric aerosol and cloud anomalies, in particular, diurnal, weekly, seasonal variations and their impact on surface insolation (Jin et al. 2005b). This is justified partly because our model is a land surface scheme and partly because modeling aerosol-cloud-land surface interaction is among the weakest components in current GCM development, and thus is not ready for implementing in our model.

The land surface energy budget is the basis for all modern land surface models:

$$(1-\alpha)S_{\downarrow} + LW_{\downarrow} - \varepsilon\sigma T_{skin}^4 + SH + LE + G = 0, \qquad (1)$$

where SH is sensible heat flux, LE is latent heat flux, G is the ground heat flux. These three processes compete for surface net radiation Rn, which is the downward minus upward shortwave and longwave radiation. In Eq. (1), α is surface albedo, and S↓ is downward solar radiation, therefore, (1-α) S↓ is reflected solar radiation. LW↓ is doward longwave radiation, and LW↑ is upward longwave radiation from the surface. Emissivity (ε) and surface skin temperature (Tskin) determine the upward longwave radiation, or surface emission, following the Stefan-Boltzmann Law. It is evident that urban modifications on α and ε play important roles in surface temperature changes since input radiative energy are changed in land surface system. In addition, the heights of buildings make the surface "roughness length" increase and thus SH and LE are affected by enhanced surface turbulence. Furthermore, urban paved roads and concrete surfaces are impervious and therefore paved surfaces lead to high Bowen ratios.

In addition to Eq. (1), which is valid for natural vegetated landscapes, urban landscapes require the introduction of two new terms in the surface energy budget: (1) anthropogenic heat flux attributed to fuel combustion, air conditioning, and other human activities (Grimmond and Oke 1999); and (2) storage heat flux due to heat emitted from vertical surfaces such as building walls (Oke 1982).

Previously, urban effects have been primarily indicated by urban-to-rural surface air temperature differences, namely the Urban Heat Island (UHI) effect (Oke 1973, Landsberg 1975). In this research, satellite land surface skin temperature is examined in addition to WMO surface air temperature measurements. Skin temperature, retrieved from upward longwave radiation, is closely related to the surface radiative properties and is more suitable than the conventional surface air temperature in studies of climate change (Jin et al. 1997, Jin and Dickinson 1999, 2000, 2002), since the latter has shortcomings as irregular spatial coverage, site changes, and coarse resolutions (Karl et al. 1988).

The following section introduces data and model we will use in this work. Section 3 discusses the urban scheme we developed. Section 4 gives model results and sensitivity studies, and final discussion and error analysis are provided in Section 5.

2. Data and Models

2.1 Satellite Observations

For the first time, we analyze MODerate resolution Spectroradiometer (MODIS) land surface skin temperature products together with corresponding surface albedo, emissivity, land cover, vegetation properties (leaf area index (LAI)), clouds and aerosol optical depths over global urban areas to quantitatively examine human-induced disturbances on the climate system. This paper, as part of our series of urban-climate studies, describes an urban model

for simulating urban heat island effects. Other results can be found in Jin et al. (2005a,b), and Jin and Shepherd (2005) for urbanization changes on albedo, emisisivity, rainfall, aerosol and clouds.

MODIS is an advanced instrument launched in May 2000 via the US NASA EOS Terra platform. This instrument simultaneously measures atmosphere, ocean, and land surface through 36 spectral bands at 1030LT (Terra) and 2230LT for a given pixel. The observations used in this study (albedo, LAI, emissivity) at nadir are 1km resolution and are scaled up to 5km for this work. Derived from surface emission, skin temperature indicates surface radiative properties and is an integrated variable related to the surface energy and water budget (Wan and Doizer 1996, Jin et al. 1997, Jin and Dickinson 1999, 2000, Jin 2004). In this work, only clear-day skin temperatures are sampled for analysis. In addition, surface emissivity is converted from MODIS spectral emissivity measurements using MODTRAN-based spectral-to-broadband equation (Jin and Liang 2004). The MODIS land cover product, with a 5-kilometer resolution, is used to divide the land surface according to the International Geosphere-Biosphere Project (IGBP) 17-class land cover types (Friedl et al., 2002). The representation of urban landscapes is improved significantly with MODIS observations (Schneider et al. 2003). The MODIS BRDF/Albedo algorithm uses a three-parameter semi-empirical RossThickLiSparse-Reciprocal BRDF model to characterize the anisotropic property of land surface reflectance (Schaaf et al., 2003, Moody et al. 2005).

2.2 NCAR CAM2/CLM2

The urban scheme developed in this work was coupled into the existing NCAR Community Land Model Version 2 (CLM2) and the Community Atmosphere Model Version 2 (CAM2). CLM2 is a community-developed land surface model. The detailed physical parameterization and numerical

implementation is given in Oleson et al. (2004). Simply put, CLM2 is designed to couple with the CAM2 atmospheric numerical model. It simulates surface albedo (direct and diffusive for visible and near-infrared spectrum), upward longwave radiation, sensible heat flux, latent heat flux, ground heat flux, water vapor flux, zonal and longitudinal stress in order to provide interactive flux boundary conditions for the overlying atmosphere model. "The model accounts for ecological differences among vegetation types, hydrological and thermal differences among soil types, and allows for multiple land cover types within one grid cell…" (Oleson et. al. 2004).

3. Urban Scheme

3.1. Physical Parameter Modifications

The first step in our development of the urban scheme is to use satellite or *in situ* observations to identify the surface physical parameters which have been modified by urbanization. In particular, these parameters include: surface albedo, surface emissivity, leaf area index, heat capacity, thermal conductivity, and hydraulic conductivity. For example, Figure 1 shows the globally averaged MODIS measured broadband albedo for various land cover types derived from the dataset of Moody et al. (2005). Evidently, urban albedo differs from other surfaces, with peak value of 0.30 at 0.9-0.12μm, while albedos for evergreen broadleaf forests and cropland are higher and needleleaf forest albedos are lower. This figure suggests that realistic albedo data is needed to properly represent the surface energy budgets when the land surface is urban. Similarly, emissivity in general decreases from that of cropland by 2-5% (not shown, see Jin et. al. 2004, Jin and Liang 2004).

As an example of MODIS-derived land cover properties and their ability to represent urban areas, Figure 2a illustrates the MODIS-derived land cover for

East Asia, including the large urban area surrounding Beijing, China. In order to better identify regions with significant UHI effects, Jin et al. (2005a) defined an "urban index" which is calculated by multiplying albedo by skin temperature. The daytime and nighttime urban indices for Beijing are outlined in Figure 2b and 2c. The unique urban heat island effect can be seen from Figures 2c and 2d, which show skin temperature over Beijing and surrounding non-urban regions, respectively. Evidently, UHI is observed for both July and January at daytime and nighttime, with a higher magnitude up-to 12°C in July daytime and 1-2°C in January night.

3.2 Urban Physical Process Representation

Two key processes that result in significant additional terms in the energy budget equation (1) must be represented in an urban scheme. These are the anthropogenic heat flux and the storage heat flux.

Anthropogenic Heat Flux (Q_f)

As discussed by Voogt and Grimmond (2000), Q_f exhibits both seasonal and diurnal variations, and may be estimated from the following equations:

$$Q_f(\text{hour}) = Q_f^0 \{1-0.6*\cos(\pi*(\text{hour}-3)/12)\}, \quad (2)$$

where, Q_f^0 = 62.5W/m^2 in January and Q_f^0 =37.5W/m^2 in July. "hour" is the hourly time of interest. In fact, Q_f^0 is function of human population density in the city as well as the style of human transport. Therefore, Q_f^0 varies with city.

Storage Heat Flux (ΔQ_s)

The storage heat flux may be represented following Arnfield (1982) and Grimmond and Oke (1999), as:

$$\Delta Q_s = \Sigma(a_i Q^* + b_i Q^s + c_i) A_i , \quad (3)$$

where a, b, and c are empirical coefficients corresponding to surface type. A_i is the surface area for each urban land surface type, which can be obtained from MODIS land cover data (Schneider et al. 2002); Q* is the net radiation; and Q^s is the absorbed surface solar radiation.

3.3 Urban Roughness Length Parameterization

Rough urban surfaces have significant impacts on the scale and intensity of turbulence, and the closely related aerodynamic conductance for momentum. A parameterization that uses height and areal fraction (λf) to calculate roughness length has been adopted from Raupach et al. (1991). The frontal index is defined by mean height (Raupach et. al. 1991):

$$\lambda f = L_y Z_H (D_x D_y) \quad (4)$$

where Dx, Dy, are the characteristic length scales of buildings as shown in Figure 4.

Following the approach provided by Macdonald et. al. (1998), and equation (4) above, we may estimate the ratio of the roughness length Zo to the average building height Z_h as:

$$Z_0/Z_h = \{(1-Z_d/Z_h)\exp[-\{0.5\beta C_d/k^2*(1-Z_d/Z_h) *\lambda f]^{-0.5}, \quad (5)$$

where Z_d is the zero-plane displacement height, C_d is a drag coefficient, k is von Karman's constant, and β is a correction factor for the drag coefficient. Macdonald et. al. (1998) showed that for staggered arrays of cubes α, β can be estimated as $\alpha = 4.43$ and $\beta = 1.0$.

4. Results

Figure 4 shows the concept of coupling urban scheme in GCM. The urban

scheme is relatively independent and therefore can be easily coupled in any existing land surface model. In a GCM/Land surface model framework, atmosphere model (in our case, CAM2) calculates atmosphere forcing that are needed by a land surface model (e.g., CLM2): surface air temperature, solar radiation, downward longwave radiation, wind, relative humidity, and precipitation. Once the land surface is called for specific grid, model needs to examine whether this grid is urban or includes urban. If yes, the newly-developed urban scheme will be called to calculate urban surface; if not, the regular land surface model will be called. Land surface model/urban scheme then calculates sensible heat flux, latent heat flux, upward long wave radiation, and reflected solar radiation and send these information back to the atmosphere model.

Offline CLM-Urban Scheme Results

Our urban scheme is first incorporated in the offline CLM2. In this case, the atmosphere forcing is from NCAR/NCAR reanalysis provided by the standard NCAR CLM2 offline package. To avoid spin-up issues, we chose the NCAR recommended restart file for initial and boundary conditions. MODIS monthly mean albedo, emissivity, and LAI data are used in the model.

The urban scheme described above was implemented first offline with CLM2 for Houston, TX, and here we present the results for a "typical" day in September 2001. Figure 5 shows that the diurnal variation of ground temperature (T_G) differs in control run (without urban scheme) and in the urban run, with the maximum around 3°C in 15:00LT, and the minimum around 1°C in middle morning (10:00LT) and early night (20:00LT). The urban scheme-simulated T_G is always larger than the control case, proving that urban physical processes result

in a net effect of improving surface ground temperature, namely the so-called UHI. In addition, both runs give reasonable diurnal cycle of T_G, suggesting the reliability of CLM2 and CLM2-urban model. Note the original diurnal range for T_G of Houston in September is about 5°C (Figure 5a), and thus an increase of 3°C due to UHI is significant.

Figure 6 shows the differences between the control run and urban-case run for 2m surface air temperature (T_{air}). The urban-induced change occurs at night, about 0.6°C at most. This may suggest one important feature of UHI, namely, urban effect on ground temperature (T_G, Fig. 5) is different from on T_{air}. For T_{air}, the urban effect is large at nighttime than at daytime, while T_G is changed by urbanization mostly at daytime. This is consistent with previously well-known UHI results: Previously, based on the WMO observed T_{air} data, UHI was found most pronounced at night, and thus UHI was considered as "nocturnal phenomena" (Oke1982). The difference between T_G and T_{air} may be caused by the physical and geometric differences of ground and 2m air layer: During the daytime of September, the ground is heated by absorbing surface insolation. The warmed surface then transports energy in sensible heat and radiative heat back to overlying air and thus heats the air there. If it existed, convection and surface layer turbulence would mix the overlying air layers and result in a negligible change in 2m T_{air}. At night, however, the stable boundary layer maintains warmed air layer and thus UHI effect is evident.

Figure 7 shows the corresponding sensible heat flux (SH). Urban effect on SH is higher during the day than that during the night, peaking around 15:00LT and minimizing at late night or early morning (5:00LT). Urbanization always increases SH because the urban human-induced surfaces (building walls, paved roads, roofs) are water-permeable, therefore less moisture available from surface. Consequently, more partitioning of absorbed solar radiation goes to SH instead

to latent heat flux (LH). During a normal day of September, the highest SH is 60Wm^{-2} – which is about a 25% increase due to urbanization.
Similarly, urbanization effects on absorbed surface solar radiation are about 8 Wm^{-2} around 15:00LT (not shown). During this day of September, the absorbed solar radiation is from up to 250 Wm^{-2}.

The upward long wave radiation (FIRA) has an increase due to urbanization-induced surface temperature increase, from 0 – 5Wm^{-2} (Figure 8), with the maximum occur at 15:00LT and late to early morning. By contrast, the ground heat flux has two low values (Figure 9): One is during the daytime afternoon, where SH is very important. The urbanization decreases ground heat flux. Another minimum time is at the late evening (24:00LT), about 10Wm^{-2}.

Single-column CAM2/CLM2-Urban Scheme Results

The UHI is a combined effect of land surface and atmosphere interaction. For the second part of our study, we execute the coupled CLM2-urban model with the CAM2 single column model, to simulate the clouds, precipitation, and surface heat fluxes over Houston for January for further examination of how urban surfaces and the atmosphere interact. Figure 10 shows one day when convective clouds and convective rainfall present. Figure 10a shows that during this cloudy day, urban effects on Tskin are not as significant as clear days: only at night just before the rainfall occurs, Tskin is slightly higher than that of non-urban case (i.e., control case). Figure 10b shows the diurnal variation of convective clouds. Urban surface increases convective clouds and shifts the peak time to a latter time of the afternoon, from 64% at 10:00LT (the 30 time steps) to 80% at 12:00 – 13:30LT (40-50 time steps), although at the 14:00LT the non-urban case had an abrupt increase in clouds amount to 100%, but only lasts for a short period of

time. Correspondingly, the convective rainfall amount increased and the peak time of the rainfall also delayed to a later time of the afternoon (Figure 10c). The height of the planetary boundary layer (PBL, Figure 10d) is increased about 100m at night, but is the same during the day partly because both cases are cloudy and thus the heat island effect is not clear during the daytime. Sensible heat flux (Figure 10e) is the same for the two cases because the Tskin change is negligible and because under a cloudy day, 2m surface air temperature is close to surface Tskin, which is consistent with previous understanding (Jin et. al. 1997, Jin and Dickinson 2000). By contrast, the latent heat flux (LE, Figure 10f) shows large differences between the urban and non-urban cases, which is related to the large differences in convective rainfall. When more rainfall occurs, the land surface soil moisture or intercepted surface waters are adequate, and thus a larger part of the absorbed solar radiation is used to evaporate water.

5. Validation

Measuring urban surface heat fluxes is extremely difficult because of the highly heterogeneous urban surface. It is still an unsolved scientific question as what is the best way to measure urban surface fluxes which can represent the integrated urban surface. Consequently, no reliable flux measurements are available to be compared with the urban scheme, which is designed to represent the integrated urban climatology instead of smaller urban sub-types (like roofs, or parking lots). Nevertheless, quantitatively we still can evaluate the model using satellite observed skin temperature for UHI. For example, for clear day, UHI is from 1°C at January night to 12°C at July day time (Figure 1), the modeled UHI is within this magnitude. In addition, satellite observations disclose the shift on urban rainfall peaking time (Brian and Shepherd 2004), which is also captured in the urban scheme (Figure 10). Such encouraging agreements suggests that, for the

first order approximation, the urban scheme may adequately represent the heat and water processes in the urban climate system.

6 Discussion

This urban scheme is developed and run both offline with the NCAR CLM2 and coupled with the single column NCAR CAM2/CLM2 to assess the mechanisms responsible for UHI. There are two-steps in our model development. First, satellite observations of albedo, emissivity, LAI, and *in situ* observed thermal properties are incorporated into the current CLM2 to represent the first-order urban effects. Second, special formulations for anthropogenic heat flux, storage heat flux, and roughness length for urban areas are included in the model. Our work suggests that human activities decrease urban surface albedo and emissivity, enhance overlying atmospheric instability and convective rainfall, and eventually result in urban heat island effect**.** Among others, albedo seems to be the most significant factor for UHI.

It has been argued that including urban areas in GCMs is not necessary because city size by itself is too small for a GCM grid cell. However, our studies (Jin et. al. 2005a) show that over large, dense urbanization regions, the size of urban regions increases dramatically to be comparable with global model grid cells. In addition, land surface models are now being coupled with GCMs as well regional climate and weather models. For example, CLM2 is coupled to CAM as well as to regional models such as MM5 and WRF (F. Chen, personal

communication 2004). Therefore the next generation of land models needs to include urban landscapes. More importantly, although a single urban region may not result in a large impact on global climate, the collective impact of all urban regions on the global climate system is as yet unknown and unstudied. Jin et al. (2004) show that zonal mean UHI has 1-3 degree warming over the Northern Hemisphere latitudes, implying that the collective UHI may be a significant contributing factor in the overall global warming signal.

One mechanism for climate change is the aggregate impact of changes in land cover or land use. Such changes are especially significant in urban areas where much of the world's population lives. This research reveals that spatial and temporal urban albedos vary dynamically as a result of human activity. As a result, reduction of albedo increases surface insolation, and consequently increases surface skin temperature. Diurnal variations of skin temperature over urban regions are also largely affected by weather conditions.

The current urban scheme does not include potentially important urban land-atmosphere feedbacks, in particular, urban aerosols' impacts on surface insolation and aerosol-cloud-rainfall interactions over urban regions. Therefore, the presented urban impacts are limited to those resulting from changes in the urban surface only. Future model development on coupled urban land-atmosphere interactions is essential for fully understanding the extent of urban impacts.

Acknowledgments. We thank the NASA/GSFC FY03 Director's Discretionary Fund (DDF), the NASA ESTO AIST NRA-02-OES-04 and EOSIDS for supporting the initial study of this work. We also thank Robert E. Dickinson for extremely useful discussion on urban roughness length. Thanks go to Dr. Michael D. King and Eric Moody for providing us MODIS land cover and albedo

data as well as to our NASA Academy summer student, Mr. Miguel Roman-Colon, who helped assess early versions of the MODIS products.

References

Arnfield, A. J., 1982: An approach to the estimation of the surface radaitive properties and radiation budgets of cities. Phys. Geogr., 3, 97-122.

Avissar, R., and R.A. Pielke, 1989: A paremeterization of heterogeneous land surfaces for atmospheric numerical models and its impact on regional meteorology. *Mon. Wea. Rev.*, **117**, 2113-2136.

Burian, S.J., Han, W.S., Velugubantla, S.P., and Maddula, S.R.K., 2003: Development of gridded fields of urban canopy parameters for Models-3/CMAQ/MM5. Final Report Prepared for Jason Ching of the U.S. Environmental Protection Agency. Department of Civil & Environmental Engineering, University of Utah, Salt Lake City, UT.

Burian, S.J. and J. M. Shepherd, 2005: Effects of Urbanization on the Diurnal Rainfall Pattern in Houston: Hydrological Processes: Special Issue on Rainfall and Hydrological Processes, 19, 1089-1103.

Changnon, S. A. 1992: Inadvertent weather modification in urban areas: Lessons for global climate change. Bulletin American Meteorological Society, 73, No. 5, 619-627.

Ek, M. B., K. E. Mitchell, Y. Lin, E. Rogers, P. Grunmann, V. Koren, G. Gayno, and J. D. Tarpley, 2003: Implementation of Noah land-surface model advances in the NCEP operational mesoscale Eta model, *J. Geophys. Res.*, 108(D22), 8851, doi: 10.1029/2002JD003296.

Friedl, M. A., D. K. McIver, J. C. Hodges, Y. Zhang, D. Muchoney, A. H. Strahler, C.E. Woodcock, S. Gopal, A. Schneider, A. Cooper, A. Baccini, F. Gao, and C.B. Schaaf, 2002: Global land cover mapping from MODIS: Algorithms and early results. *Remote Sensing Environ.*, **83**,287-302.

Grimmond, C. S. B. and T. R. Oke, 1995: Comparison of heat fluxes from summertime observations in the suburbs of four North American cities. *Journal of Applied Meteorology, 34*, 873-889,.

Grimmond, C. S. B. and T. R. Oke, 1999: Heat storage in urban areas: Local-scale observations and evaluation of a simple model. J. Appl. Meteor., 38, 922-940

Hansen, J., R. Ruedy, M. Sato, M. Imhoff, W. Lawrence, D. Easterling, T. Peterson, and T. Karl, 2001: A closer look at United States and global surface temperature change. *J. Geophy. Res.*, **106** (D20), 23,947-23,963.

IPCC, Intergovernmental Panel on Climate Change, *Climate Change* 2001: *The Scientific Basis. Contribution of working group 1 to the Third Assessment Report of the Intergovernmental Panel on Climate Change*, edited by J. T. Houghton et. al., 881 pp., Cambridge Univ. Press, New York,.

Jin, M., 2004: Analyzing skin temperature variations from long-term AVHRR, *Bull. Amer. Meteor. Soc.*, 587-600,.

Jin, M., and R. E. Dickinson, 2002: New observational evidence for global warming from satellite data, *Geophys. Res. Lett., 29(10),* doi:10.1029/2001GL013833.

Jin, M., and J. M. Shepherd, 2005: On including urban landscape in land surface mode—How can satellite data help? *Bull. Amer. Meteor. Soc.*, *86*, in press.

Jin, M. and S. Liang, 2004: Improving Land Surface Emissivity Parameter of Land Surface Model in GCM. Conditionally accepted by Journal of Climate.

Jin, M., R. E. Dickinson, and D. Zhang, 2005a: The footprint of urban climate change through MODIS, In press by *J. Climate*. 2005a.

Jin, M., J. M. Shepherd, and M. D. King, 2005b: Urban aerosols and their interaction with clouds and rainfall: A case study for New York and Houston. *J. Geophys. Res.*, submitted.

Karl, T. R., H. F. Diaz, and G. Kukla, 1988: Urbanization: Its detection and effect in the United States Climate Record, *J. Climate*, *1*, 1099-1123.

King, M. D., W. P. Menzel, Y. J. Kaufman, D. Tanré, B. C. Gao, S. Platnick, S. A. Ackerman, L. A. Remer, R. Pincus, and P. A. Hubanks, 2003: Cloud and aerosol properties, precipitable water, and profiles of temperature and humidity from MODIS, *IEEE Trans. Geosci. Remote Sens.*, *41*, 442-458.

Linacre, E., and B. Geerts, 2002: Estimating the annual mean screen temperature empirically, *Theor. Appl. Climat.*, *71*, 43-61.

Mace, G. G., Y. Zhang, S. Platnick, M. D. King, P. Minnis, and P. Yang, 2004: Evaluation of cirrus cloud properties derived from MODIS radiances using cloud properties derived from ground-based data collected at the ARM SGP site, *J. Appl. Meteor.*, in press,.

Macdonald, R. W., R. F. Griffiths, and D. J. Hall, 1998: An improved method for estimation of surface roughness of obstacle arrays. Atmos. Environ., 32, 1857-1864.

Moody, E. G., M. D. King, S., Platnick, C. B. Schaaf, and F. Gao, 2005:Spatially complete global spectral surface albedos: Value-added datasets derived from Terra MODIS land products. IEEE Trans. Geosci. Remote Sens., 43, 144-158.

Oleson, K.W., et al., 2004: Technical Description of the Community Land Model(CLM), NCAR Technical Note NCAR/TN-461+STR, National Center for Atmospheric Research, Boulder, Colorado 80307-3000, 173 pp.

Oke, T. R., 1976: City size and the urban heat island. *Atmos. Environ.,* **7**, 769-779, 1976.

Oke, T. R., 1982: The energetic basis of the urban heat island, *Quart. J. Roy. Meteor. Soc.*, *108*, 1-24, 1982.

Otte T. L., A. Lacser, S. Dupont, and J. K-S. Ching, 2004: Implementation of an

urban canopy parameterization in a mesoscale meteorological model, *J. App. Met.* 43 (11): 1648-1665.

Raupach, S. 1992: Drag and drag partition on rough surfaces. *Bound.-Layer Meteo*. 60,375-395.

Schaaf, C. B., and Co-authors, 2003: First Operational BRDF, Albedo and Nadir Reflectance Products from MODIS. *Remote Sens. Environ.* In press.

Shepherd, J. M., and S. J. Burian, 2003: Detection of urban-induced rainfall anomalies in a major coastal city, *Earth Interactions*, 7(4), doi:10.1175/1087-3562(2003)007, 2003.

Shepherd, J. M., H. Pierce, and A. J. Negri, 2002: Rainfall modification by major urban areas: Observations from spaceborne rain radar on the TRMM satellite, *J. Appl. Meteor.*, *41*, 689-701.

Schneider, A., M. A. Friedl, D. K. McIver, and C. E. Woodcock, 2002: Mapping urban areas by fusing multiple sources of coarse resolution remotely sensed data. *Photogramm. Eng. Remote Sens.*, **69**, 1377-1386.

Voogt, J. A. and C. S. B. Grimmond, 2000: Modeling surface sensible heat flux using surface radiative temperatures in a simple urban area. J. of Applied Meteorology, 39, 1679-1699.

Wan, Z., and J. Dozier, 1996: A generalized split-window algorithm for retrieving land-surface temperature from space. *IEEE Trans. Geo. Remote Sens.*, **34**, 892-904.

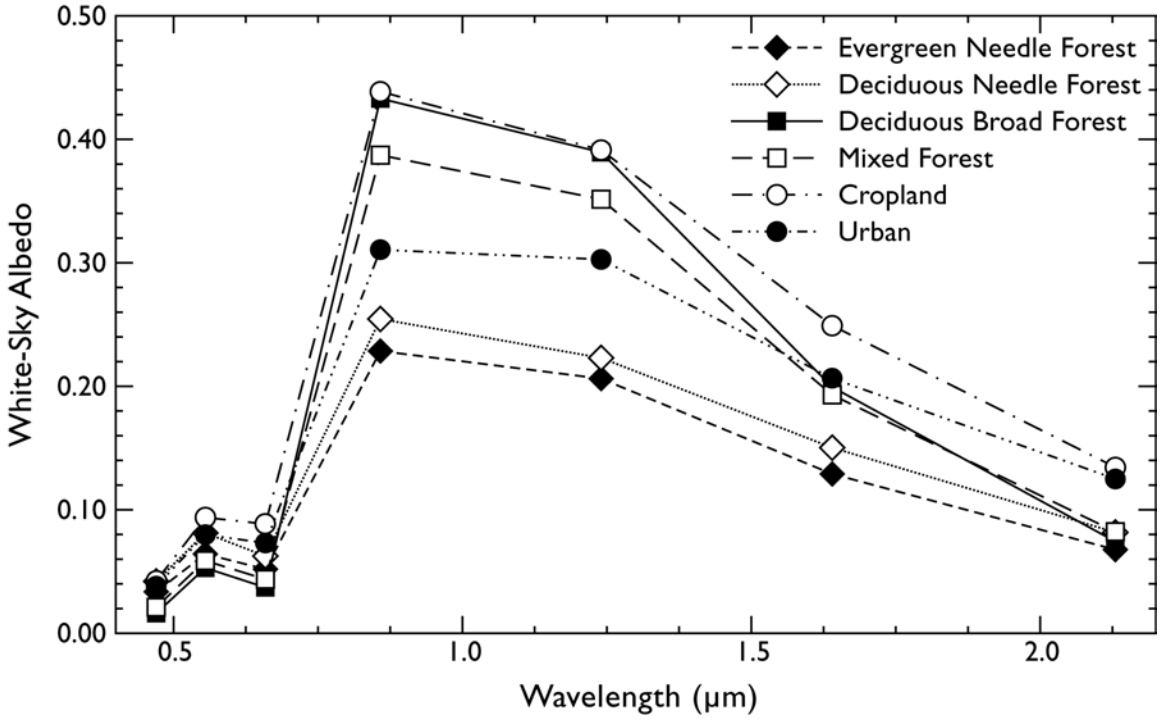

Figure 1: MODIS observed annual surface albedos for certain land covers based on Moody et al. (2005).

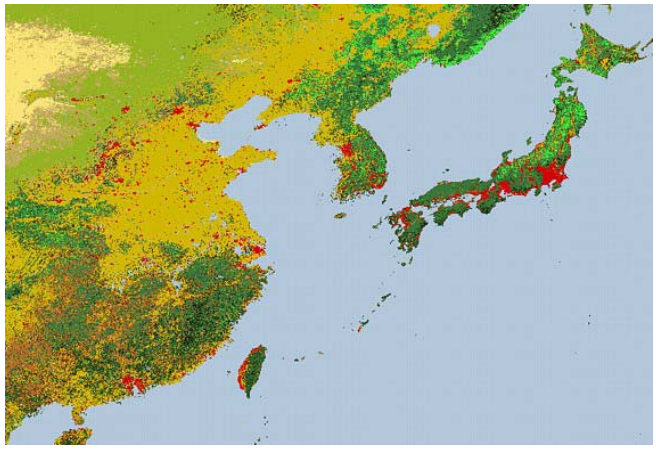

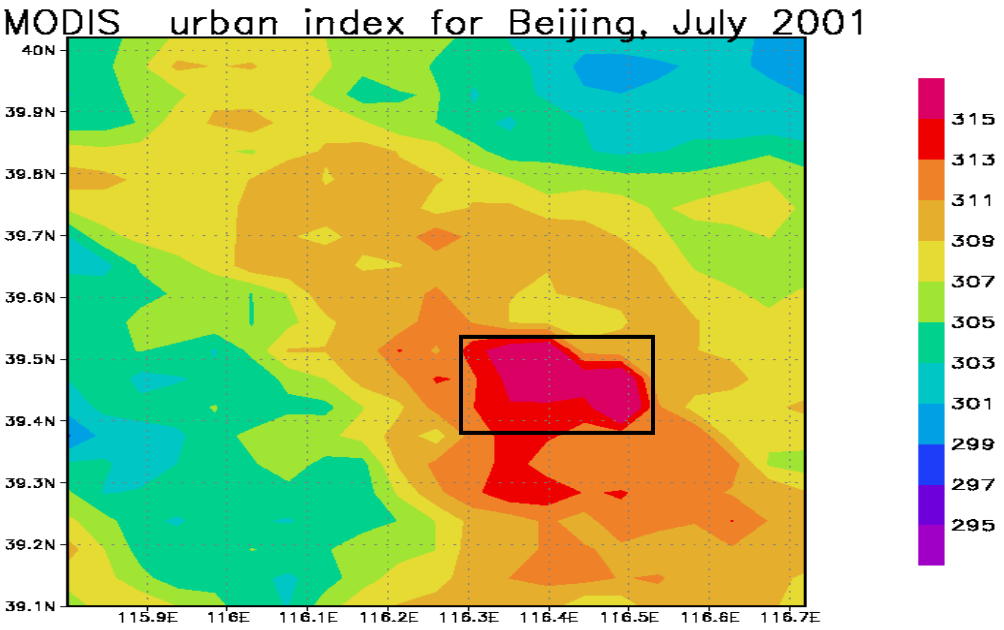
MODIS urban index for Beijing, July 2001
40N
39.9N
39.8N
39.7N
39.6N
39.5N
39.4N
39.3N
39.2N
39.1N
115.9E
116E
116.1E
116.2E
116.3E
116.4E
116.5E
116.6E
116.7E
315
313
311
309
307
305
303
301
299
297
295

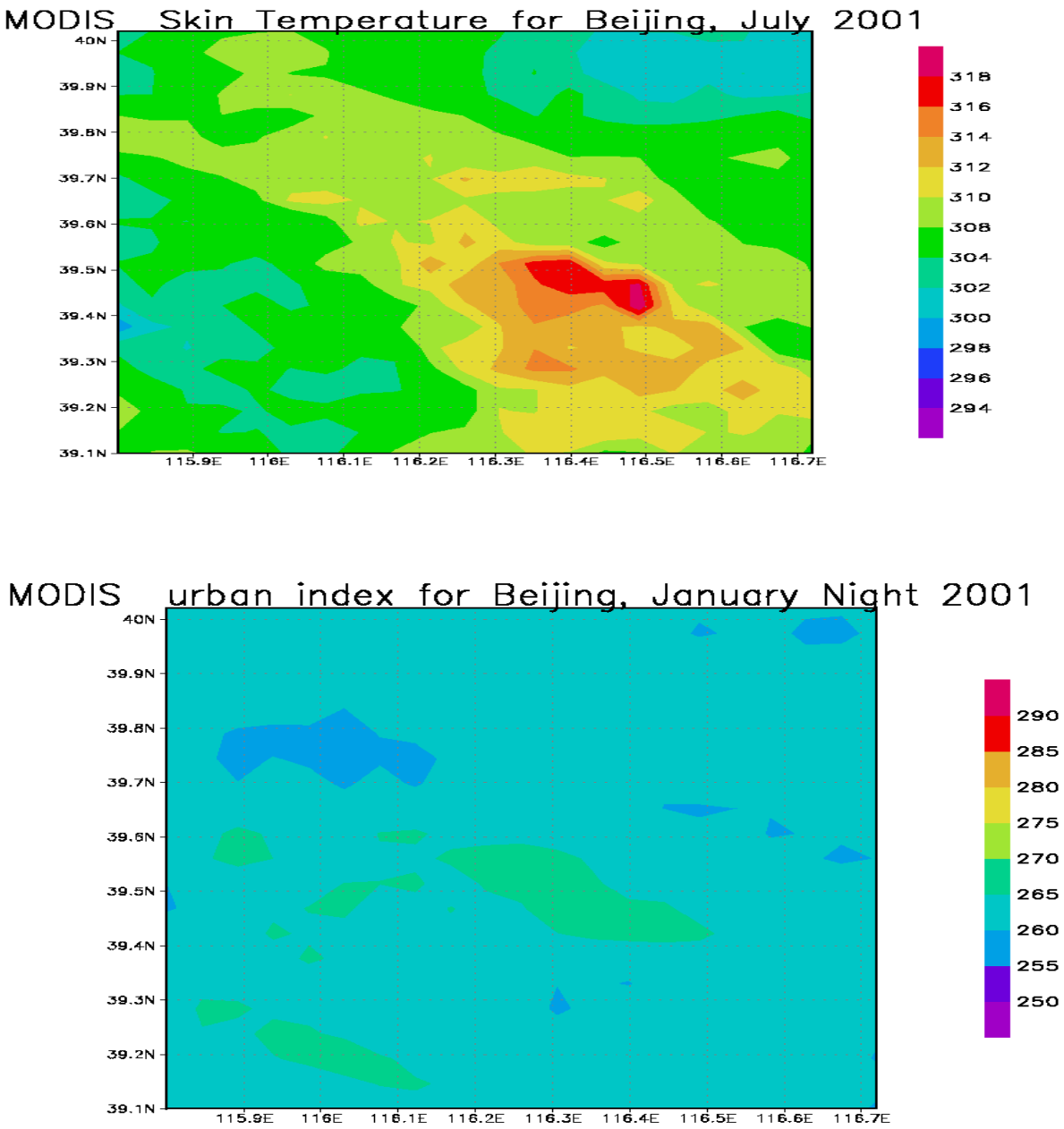

Figure 1: (a) Examples of MODIS observed land cover for East Asia, including urban. This figure is provided by Michael D. King. (b) The urban index, defined as skin temperature times (1-albedo). Urban index is defined in Jin et. al. (2005) to better identify urban heat island effect over urban regions. (c) Urban skin temperature for Beijing region for July 2001, daytime. (d) Urban heat island effect for Beijing January 2001, nighttime.

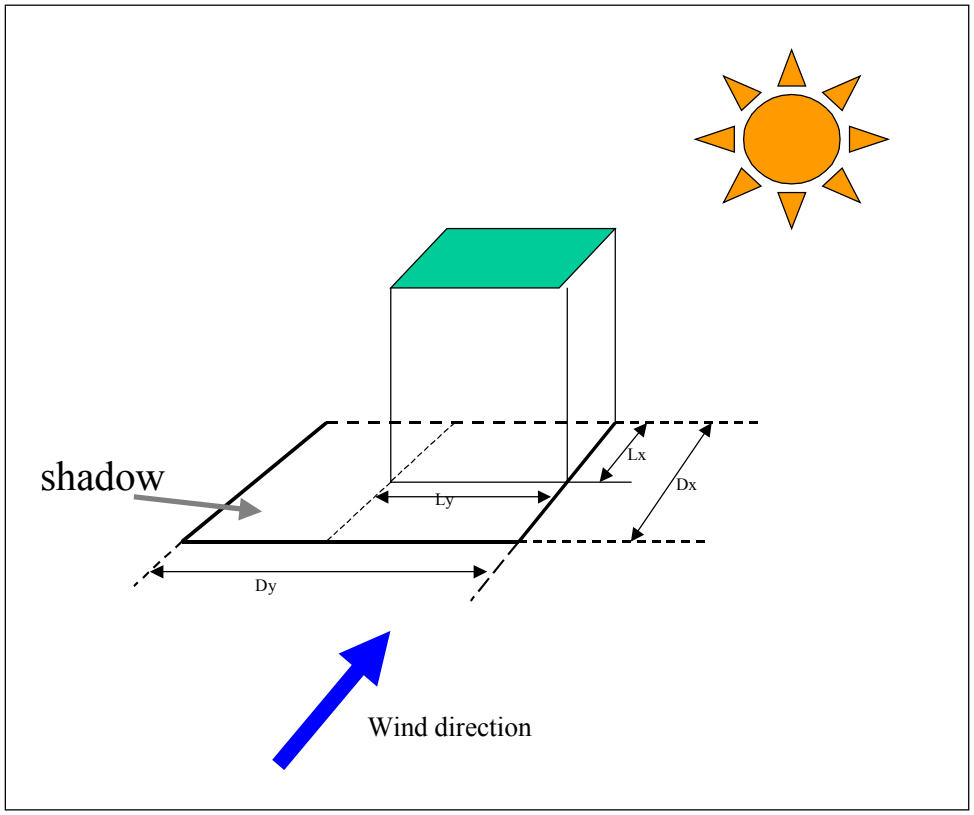

Figure 3: Definitions of building length used in Equation (4).

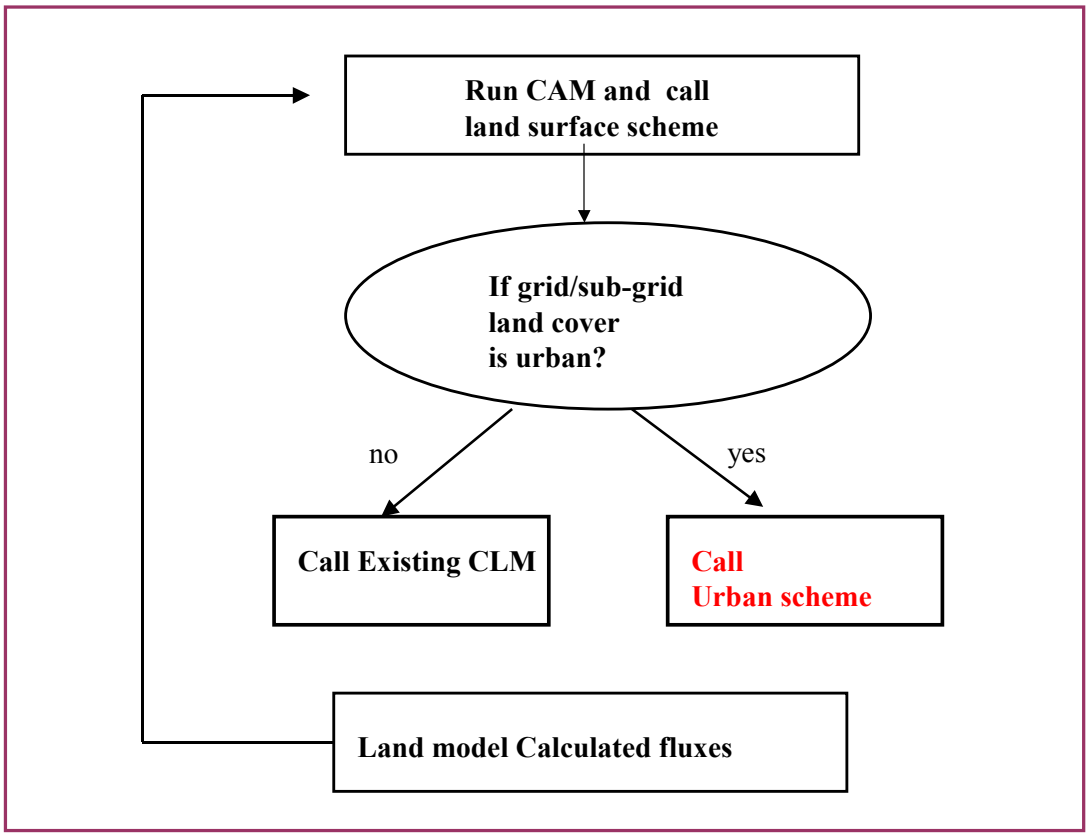

Figure 4. The data flow of urban scheme coupled with CAM2/CLM2. See text for details.

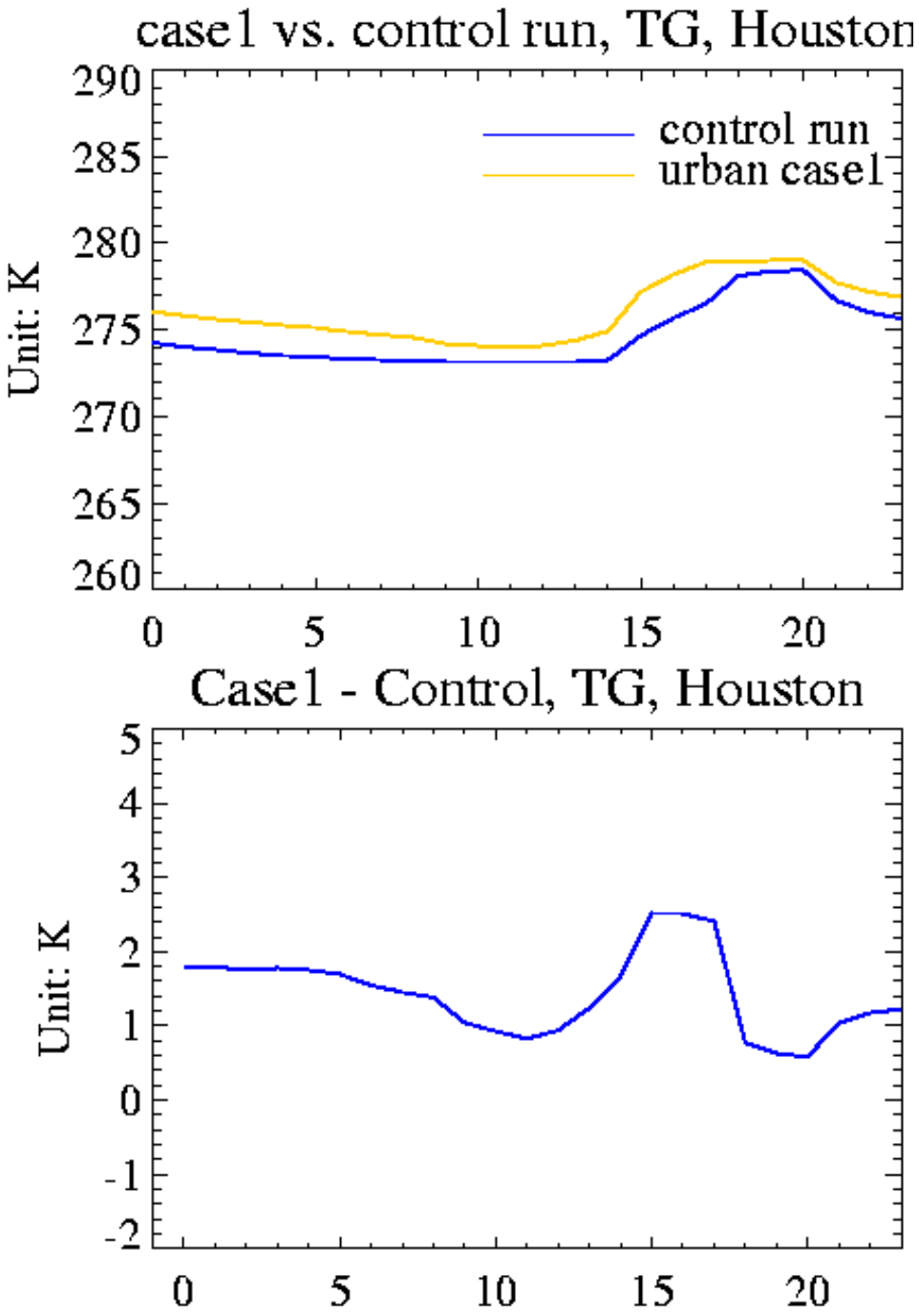

Figure 5. (a): Diurnal cycle of surface air temperature simulations from offline CLM2-urban model. "Case 1" is the run with urban scheme, and "control run" is the CLM2 without urban scheme. (b) is the differences between case 1 and control runs. The day is one random day in September.

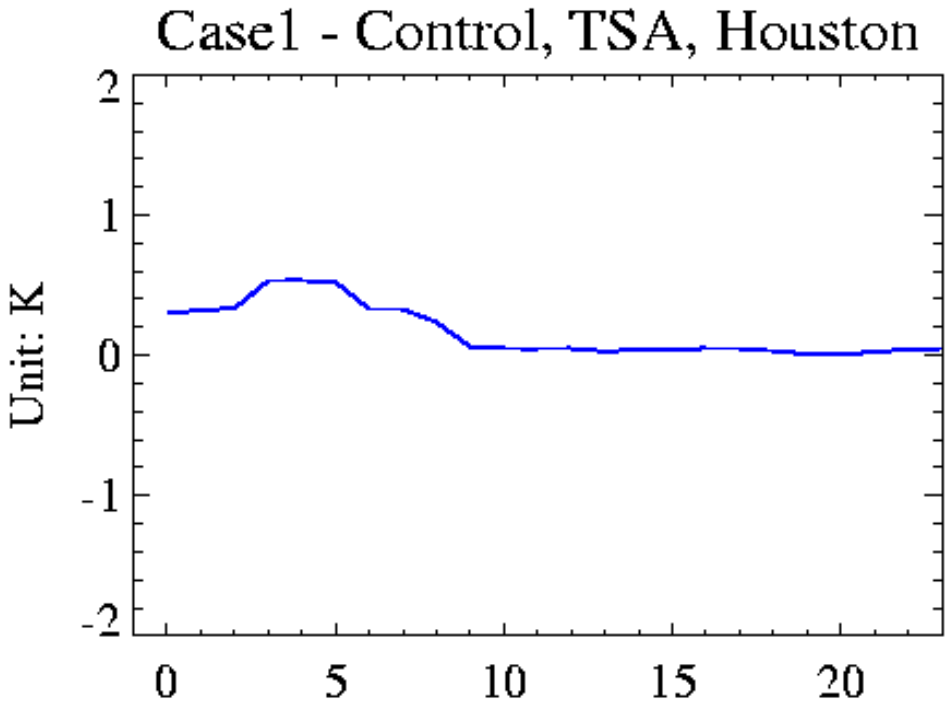

Figure 6. The differences of surface air temperature simulations from offline CLm2-urban model. "Case 1" is the run with urban scheme, and "control run" is the CLm2 without urban scheme.

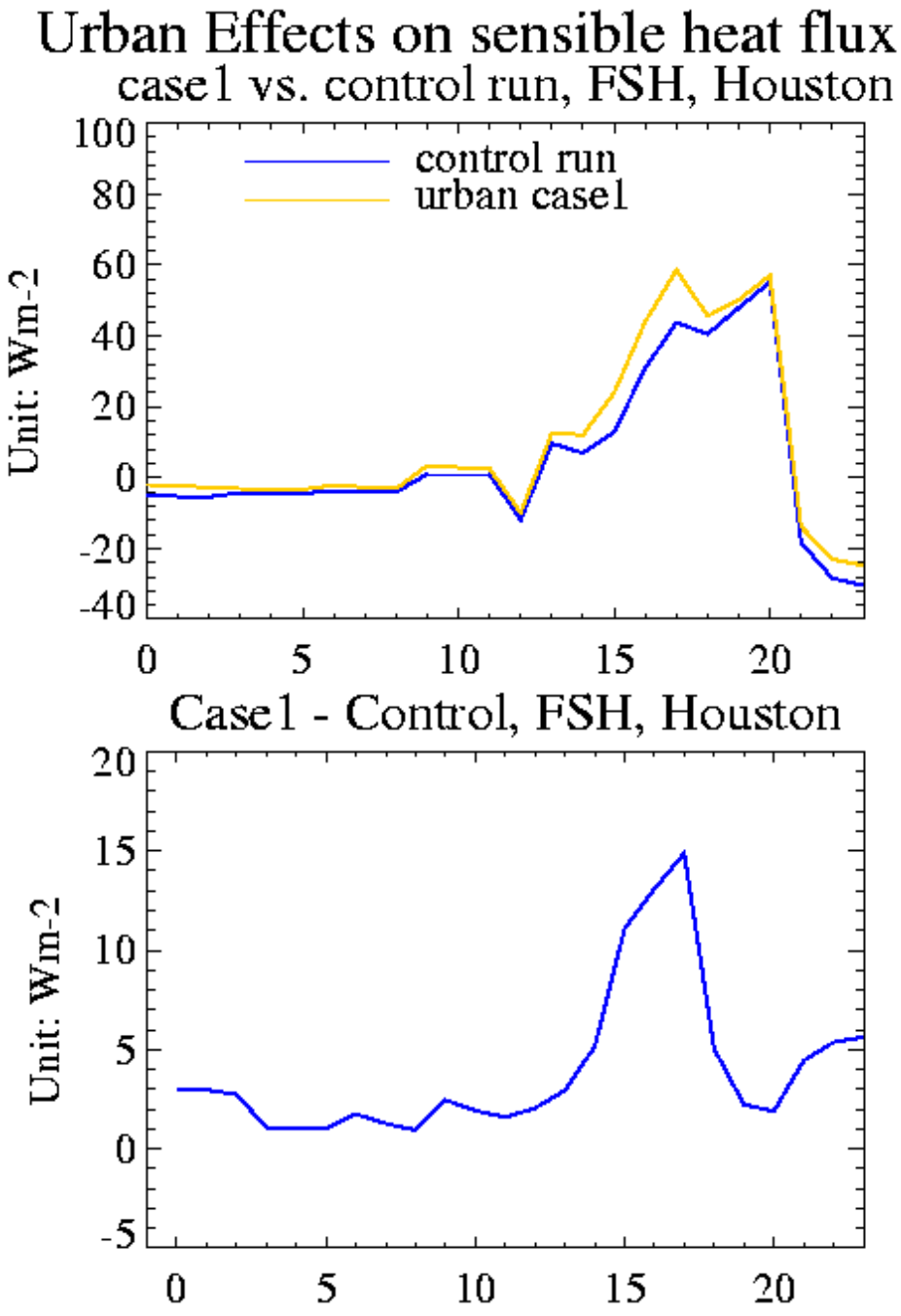

Figure 7: Same as Fig. 5, except for sensible heat flux.

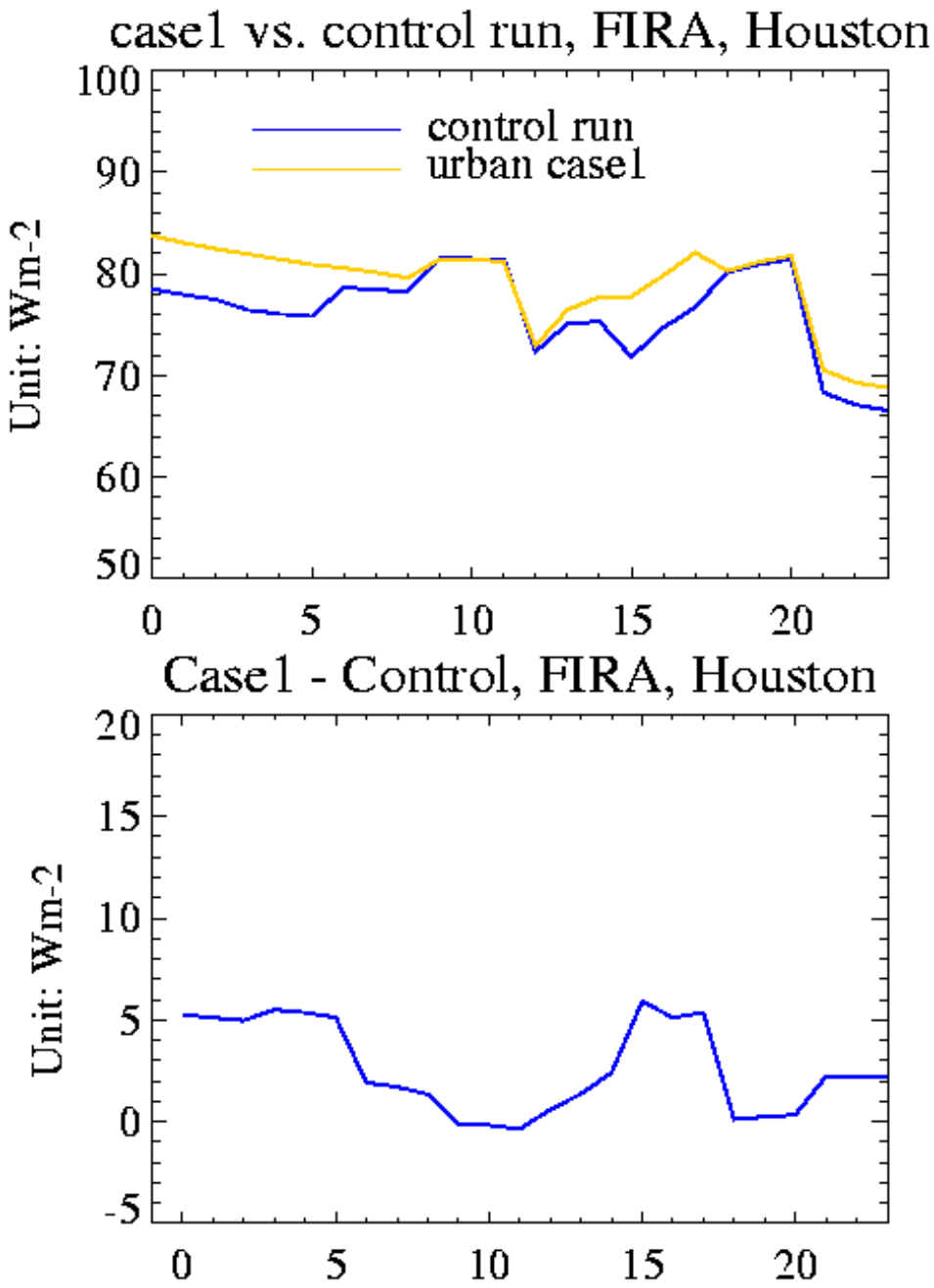

Figure 8. Same as Figure 7, except for net longwave radiation.

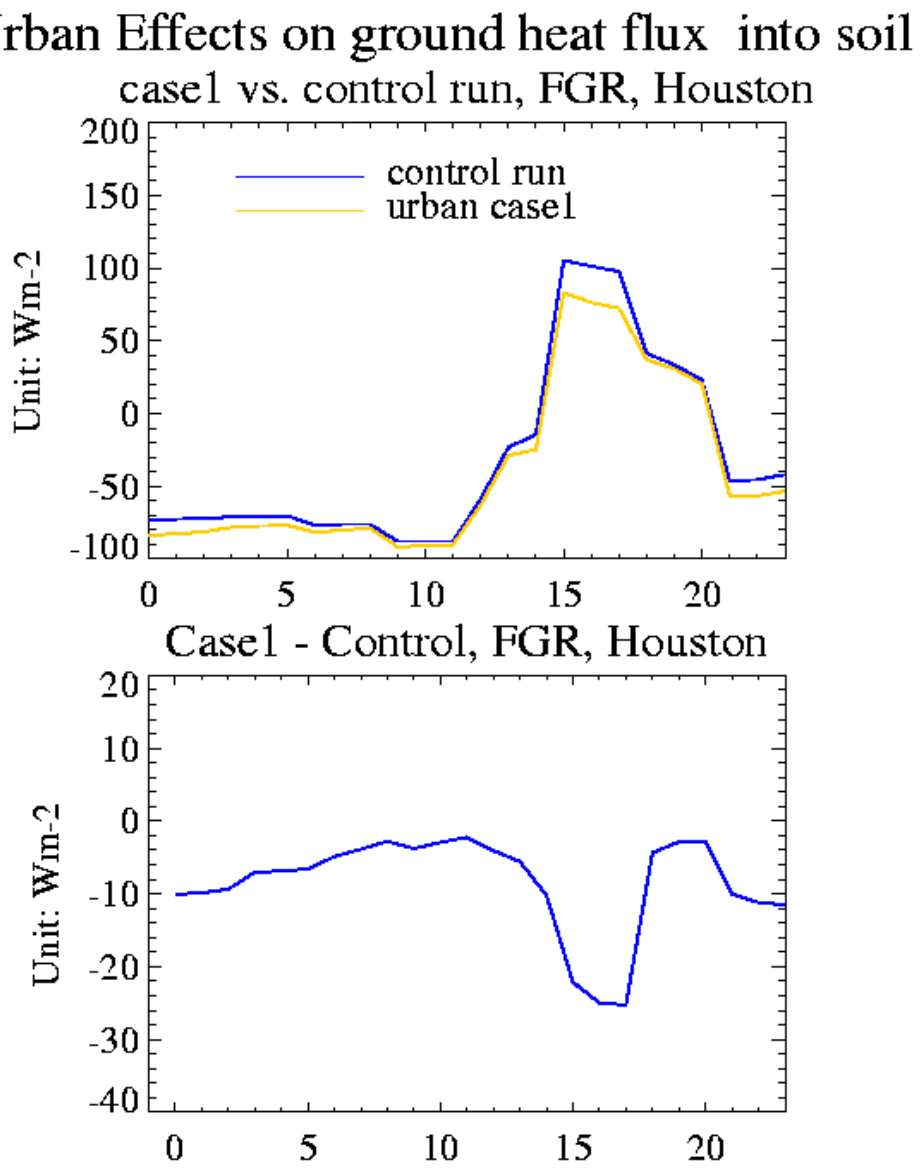

Figure 9: Same as Figure 8, except for ground heat flux.

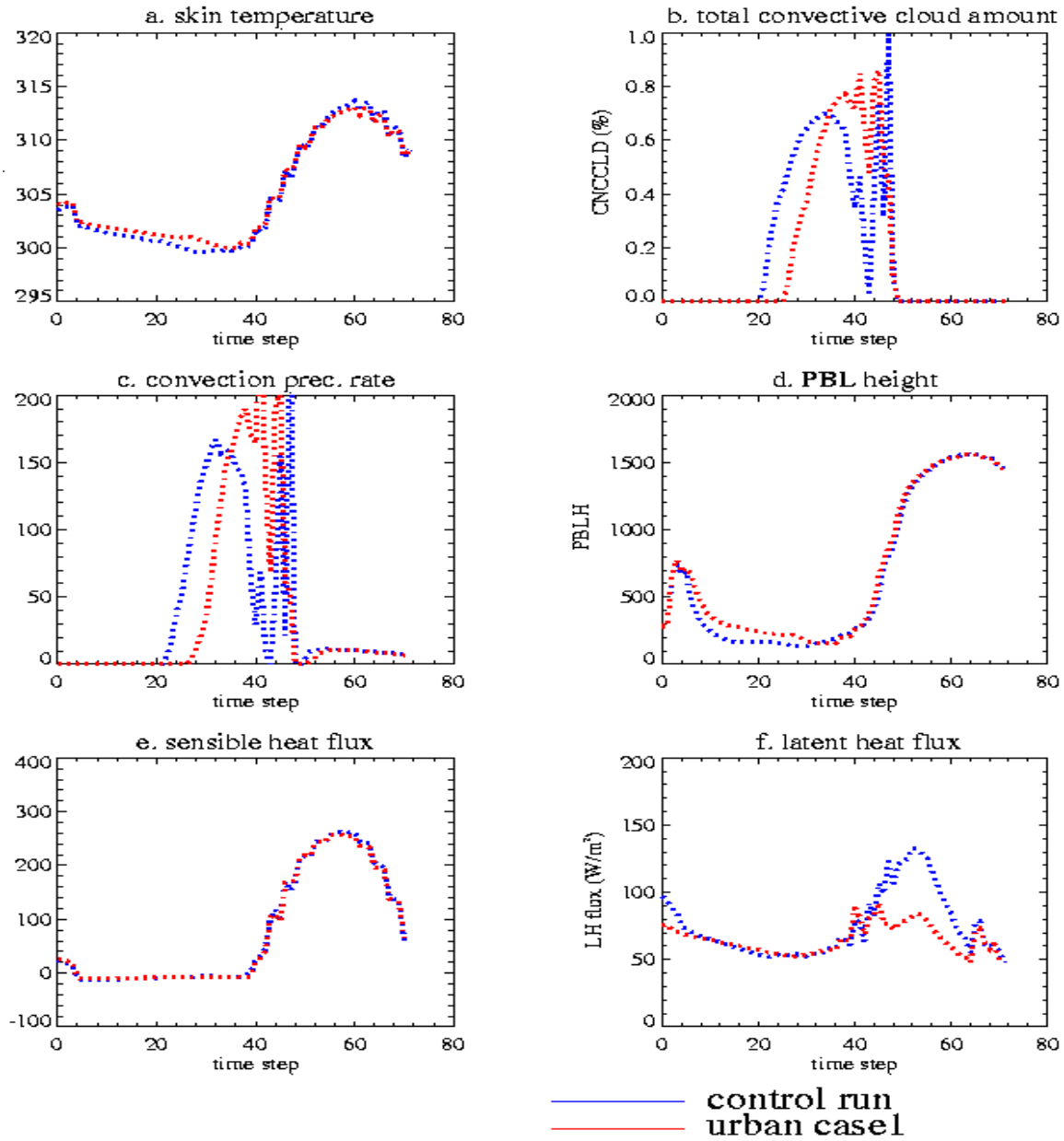

Figure 10. Urban effects simulated from single column model of NCAR CAM2/CLM coupled with urban scheme: (a) Land surface skin temperature, (b) total convective cloud amount; (c) convection precipitation rate; (d) PBL height; (e) sensible heat flux; (f) latent heat flux.